Adaptive Design of Experiments for Efficient and Accurate Estimation of Aerodynamic Loads

Andrea Da Ronch[a,*], Marco Panzeri[b], M. Anas Abd Bari[a], Roberto d'Ippolito[b], Matteo Franciolini[c]

[a] *Faculty of Engineering and the Environment, University of Southampton, Southampton, SO17 1BJ, U. K.*
[b] *Noesis Solutions N. V., 3001 Leuven, Belgium*
[c] *Dipartimento di Ingegneria Industriale e Scienze Matematiche, Universitá Politecnica delle Marche, I–60100, Ancona, Italy*

Abstract

Aerodynamic design, which aims at developing the outer shape of the aircraft while meeting several contrasting requirements, demands an accurate and reliable aerodynamic database. Computing forces and moments with the highest level of fidelity is a prerequisite, but practically limited by wall clock time and available computing resources. An efficient and robust approach is therefore sought after. This study investigates two design of experiments algorithms in combination with surrogate modelling. In traditional design of experiments, the samples are selected *a priori* before running the numerical explorative campaign. It is well–known that this may result in either poor prediction capabilities or high computational costs. The second strategy employs an adaptive design of experiments algorithm. As opposed to the former, this is a self–learning technique that iteratively: i) identifies the regions of the design space that are characterised by stronger non–linearities;

*First corresponding author. Email: A.Da-Ronch@soton.ac.uk

and ii) select the new samples in order to maximise the information content associated with the simulations to be performed during the next iteration. In this work, the Reynolds–averaged Navier–Stokes equations are solved around a complete aircraft configuration. A representative flight envelope is created taking the angle of attack and Mach number as design parameters. The adaptive strategy is found to perform better than the traditional counterpart. This is quantified in terms of the sum of the squared error between the surrogate model predictions and CFD results. For the pitch moment coefficient, which shows strong non–linearities, the error metric using the adaptive strategy is reduced by about one order of magnitude compared to the traditional approach. Furthermore, the proposed adaptive methodology, which is employed on a high performance computing facility, requires no extra costs or complications than a traditional methodology.
Keywords: design of experiments, adaptive sampling, surrogate model, computational fluid dynamics, transonic cruiser, turbulence model

1. Introduction

Accurate predictions of aerodynamic loads are generally needed as early as possible during the aircraft design process. For a number of flight conditions prescribed by certification authorities, aerodynamic loads form a set of critical loads that are used to size aircraft structural components. It is critical to limit the uncertainty associated with critical aerodynamic loads because: i) if the critical loads are underestimated, as revealed following flight test, then expensive re–design is often required incurring the costs and penalties arising from programme delay; and ii) if the critical loads are overestimated,

the aircraft will be heavier than needed with degraded performances.

Traditionally, the aircraft design process relies heavily on semi–empirical relations and linear assumptions. The reason for this is that, at the early stage of the design process, designers explore a large parameter space resulting in a large number of numerical evaluations. Speed requirements dominate over accuracy. As the design parameters are tightened and addressed in increasing detail, the need for improved realism of predictions calls for higher fidelity aerodynamic models. Despite the availability of high performance computing (HPC) facilities, the routine use of computational fluid dynamics (CFD) is limited to academic demonstrations. The reasons that linear methods have cornered the industrial aircraft design process are two–fold. First, linear methods are corrected to account for un–modelled flow physics. Corrections have been calibrated using a number of previous aircraft configurations, and high confidence exists. The second reason is that linear methods are fast enough for parametric searches, and their analysis setup is straightforward practically building on a simplified description of the lifting surfaces.

The work presented in this paper addresses the problem to efficiently use CFD as source of the aerodynamic predictions. For a representative parameter space, the problem consists of maximising the information extracted from a limited number of CFD analysis. Several techniques are nowadays available in order to design the virtual experimental campaigns in an efficient and effective way. These include: i) orthogonal design techniques (e.g. fractional, full–factorial), in which the design points are chosen deterministically before running the virtual experiments; and ii) random methods (e.g. Monte Carlo

sampling, Latin Hypercube), where the location of the design points is chosen randomly. The main limitation associated with traditional orthogonal and random design of experiments (DOE) techniques lies in the fact that the samples to be evaluated are chosen all at the same time, based only on information that is available before running the numerical explorative campaign. Since the knowledge available before running the DOE is often very limited, this approach makes impossible to know in advance the optimal number of samples and the location of the design points that are required in order to achieve a given accuracy in the response surface model built upon the results of the virtual experiments. A possible problem arising in this context is the so–called under–sampling effect, where the number of design points and their locations do not provide sufficient information to build a response surface function with the desired level of accuracy. This behaviour is typically observed when design points are not distributed with sufficient density in those regions of the parameter space where the output model is characterised by a pronounced non–linearity. The opposite effect, named over–sampling, is encountered when the level of accuracy associated with the response surface model could have been achieved by running a smaller number of experiments. This happens, for example, when the distribution of the design points is too dense and leads to unnecessary and avoidable computational burdens.

A feasible way to mitigate the appearance of these problems consists of adopting a more advanced algorithm, such as the adaptive DOE (ADOE). This a self–learning algorithm which makes use of an iterative procedure and is capable to: i) identify from previous runs the regions of the design space where the output model is characterised by stronger non–linearities;

and ii) select a new batch of design points by maximising the (expected) information content associated with this new set of simulations. Previous applications of ADOE techniques to CFD problems can be found in Ref. (1; 2; 3). In this work, we propose to employ an ADOE methodology to identify the locations of CFD analyses that provide the best approximation of the objective function. The test case is for a complete aircraft configuration which is run on the HPC of the University of Southampton [1].

The paper continues in Section 2 over–viewing the aircraft configuration used as test case. Section 3 provides a description of the CFD solver, the turbulence model, and the computational grid. Then, Section 4 describes the DOE algorithms employed in this work. Results are discussed in Section 5, where the proposed methodology is compared with current state–of–the–art methods. Finally, conclusions are drawn in Section 6.

2. Test Case

The test case is for the transonic cruiser (TCR) model that was conceived during the SimSAC (Simulating Aircraft Stability and Control Characteristics for Use in Conceptual Design) project (4). The TCR is a conceptual design of a civil transport aircraft operating at a target Mach number of 0.97, featuring low relaxed static stability boundaries, and low manoeuvre and trim drag. The initial concept proposed by SAAB was for a conventional tailed configuration, which revealed the need for a large horizontal tail

[1]IRIDIS at the University of Southampton is in the World's Top500 ranking and is the largest HPC facility in the U. K. after the national supercomputer. In total, it consists of 12320 processor–cores providing 250 TFlops peak.

deflection affecting significantly trim drag. The evolution from the initial geometry to the final configuration, which includes an all–moving canard for longitudinal control, may be found in Ref. (5).

A wind tunnel model of the TCR aircraft was built in a 1:40 scale compared to the full scale aircraft. A schematic of the TCR design and the sign convention adopted in this work are shown in Figure 1. The apex positions of the canard and main wing are, respectively, at 12 and 26% of the fuselage length. The close proximity of the canard with the main wing originates strong interference effects of the flow past the canard impinging on the main wing.

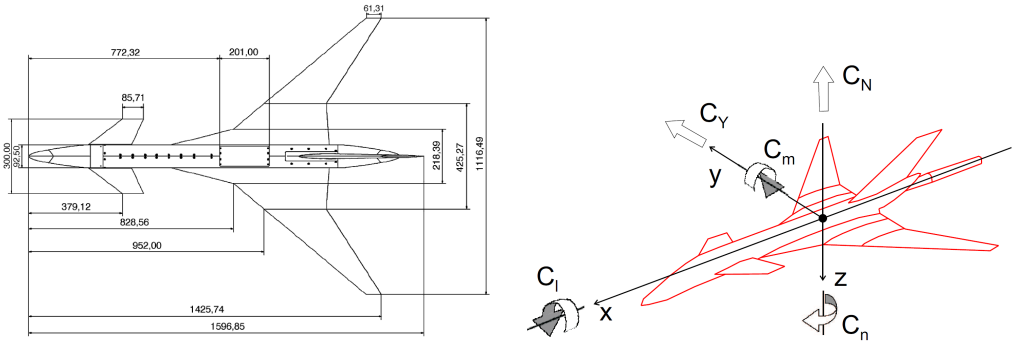

(a) TCR model top view (b) Body frame of reference

Figure 1: TCR wind tunnel model

Numerical analyses presented in this work were obtained for the TCR wind tunnel model geometry. Reference values are summarised in Table 1. The geometry features a symmetric aerofoil for the canard, and a cambered one for the main wing. The moment reference point is measured from the aircraft nose, positive downstream.

Table 1: Reference values of the TCR wind tunnel model

Parameter	Value
Model scale	1:40
Reference area	0.3056 m^2
Wing span	1.12 m
Mean aerodynamic chord	0.2943 m
Moment reference point	0.87475 m
Fuselage length	1.597 m

2.1. Experimental Investigations

Experimental investigations of the steady and unsteady aerodynamic characteristics at low speed were performed in the T–103 wind tunnel facility at the Central Aerohydrodynamic Institute (TsAGI), see Figure 2. The wind tunnel has an open jet working section of the continuous type with an elliptical cross section, 4.0 m $\times$ 2.33 m. Several configurations of the wind tunnel model were tested to evaluate the influence of single components (vertical tail and canard wing) on the overall performance. The experimental measurements included the investigation of the static aerodynamic characteristics, rotary and unsteady aerodynamic derivatives, and unsteady non–linear aerodynamic characteristics during large amplitude oscillations. The normal and lateral force and moment coefficients from static and large amplitude oscillations were measured. The mean values and in–phase and out–of–phase components of the force and moment coefficients were measured in forced motions. The full dataset of wind tunnel measurements is described in Ref. (6).

(a) Canard–off configuration (b) Canard–on configuration

Figure 2: Wind tunnel model of the TCR tested in TsAGI; (a) large amplitude pitch oscillations dynamic rig, and (b) 90 deg bank angle for static aerodynamic characteristics

It is worth noting that no transition tripping was installed in the wind tunnel model, and that the leading edge of all lifting surfaces is round. As discussed below, the combination of these two aspects makes the prediction of the TCR aerodynamic characteristics challenging from a numerical standpoint. It is well–known that the vortical flow behaviour around delta wings with a round leading edge is significantly different from that around wings with a sharp leading edge (7). The separation line is fixed for a sharp leading edge, but depends highly on Reynolds number, surface roughness, leading edge bluntness and sweep angle for a round leading edge. Wind tunnel tests were run at a freestream speed of 40 m/s, which corresponds at sea level to a Mach number of 0.117 and a Reynolds number of 0.778 million, based on the mean aerodynamic chord of the wind tunnel model.

2.2. Numerical Investigations

Numerical investigations reported in Refs. (2; 8; 9) focussed at comparing steady and unsteady predictions of the aerodynamic loads with available experimental measurements. Reference (8) employed a modified version of the k–ω turbulence model and a multi–block structured grid with 8.5 million grid points. Predictions for steady results were first validated. The attention was then addressed for unsteady aerodynamics. Numerical results of aerodynamic derivatives for small oscillation amplitudes were presented, followed by results for large amplitude motions. Dependencies of dynamic characteristics on mean angle of attack and reduced frequency were investigated. Computations were for the wind tunnel model with vertical tail and un–deflected canard wing. To the authors' knowledge, this is the only original work that performed unsteady time domain calculations based on Reynolds–averaged Navier–Stokes (RANS) modelling to extract dynamic derivatives. In Ref. (9), experimental and numerical research activities for the determination of dynamic derivatives were reviewed for two aircraft configurations, including the TCR model. In addition to the unsteady RANS (URANS) results of Ref. (8), the reference included results from linear aerodynamic models based on a panel method. Reference (2) discussed current state–of–the–art methods to generate aerodynamic tables for flight simulation. For the TCR model, the ability to combine aerodynamic databases of different fidelity levels into a single database was demonstrated. In total, 270 CFD simulations were run, and combined with linear aerodynamics that provided quantitative trends of the aerodynamic loads across the flight envelope at very low computational cost.

3. Computational Fluid Dynamics Solver

The flow solver used in this work is Ansys Fluent (version 14.5). The reason to use a commercial solver, opposed to previous work done by the first author with research codes, is to demonstrate the seamless integration of the ADOE methodology with a well–established software tool. We hope this demonstration will facilitate the adoption of the ADOE methodology in the analysis of other complex and non–linear engineering phenomena.

The low Reynolds number of the operating wind tunnel conditions ($M = 0.117$ and $\mathrm{Re} = 0.778 \cdot 10^6$) and the blunt leading edge geometry of the TCR wind tunnel model make the prediction of the resulting turbulent flow difficult, especially for what concerns the flow separation near the wing leading edge. No transition tripping was used in the wind tunnel model. Without other information, all simulations herein reported were run assuming fully turbulent flow. The one–equation Spalart–Allmaras turbulence model was used in this study. The model provides the turbulent viscosity to be added to the viscous terms of the Navier–Stokes equations and mimics the effects of the inertial turbulent transport on the mean flow. The details of the turbulence model can be found in Ref. (10). All computations were run in double precision.

An unstructured grid for the half–model configuration was generated with 10 million points. Jobs were run on IRIDIS on 32 processes and about 10 hours of wall clock time. The flow field has a semi–spherical shape with the far–field located on average at 170 times the mean aerodynamic chord from the aircraft geometry. This ensures avoiding that the flow field disturbances propagate beyond the far–field boundary. Boundary conditions were set to

symmetry plane on the vertical plane of symmetry, and to no–slip adiabatic wall on the aircraft surface. At the inlet, the pressure gradient was set to zero while the flow velocity set to the free–stream conditions. The grid, show in Figure 3, was chosen after a grid convergence study was carried out, demonstrating independence of the results obtained with the currrent grid size.

In all cases, computed results are for zero side–slip angle and the influence of the rear sting was ignored. The moment reference point is set at 54.78% of the fuselage length from the foremost point.

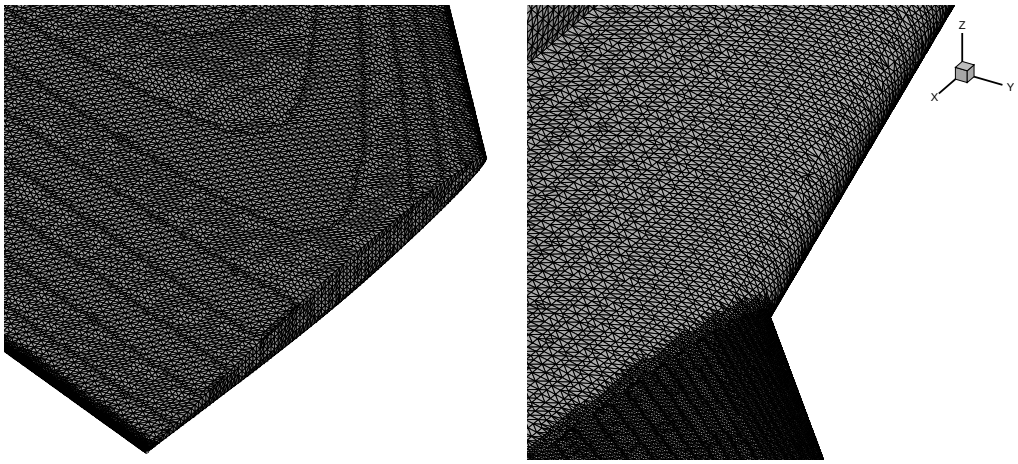

(a) Canard wing tip (b) Kink on main wing

Figure 3: Surface grid of the TCR wind tunnel model

4. Design of Experiments

For the size of the computational grid used in this work, a well–converged simulation is computed at high computing times. The generation of the aerodynamic database across the flight envelope adopts an ADOE technique.

A detailed description of the ADOE algorithm is given in Section 4.1, and a review of the Latin–Hypercube (LH) method in Section 4.2. The latter is used as benchmark in order to assess the improvements achieved by the ADOE technique compared with a more traditional, industry–standard DOE method.

4.1. Adaptive Design of Experiments

The ADOE is an iterative DOE technique in which the data produced during previous iterations are analysed in order to distribute the design points of the next iteration in areas of the parameters space considered of interest only. The ADOE is a self–learning algorithm that is driven by two opposite factors: space–learning and feature–learning.

Space–learning is the act of exploring the domain to find areas of the design space that have not yet been explored. The main goal of space learning is to fill the design space uniformly, avoiding the need of any information about the response of the model. Maximin sampling (11) is the technique implemented to support the space–learning aspect of our ADOE algorithm. Conversely, the goal of feature–learning is to add new samples in areas of the domain that have already been identified as interesting for some reason. Feature–learning is then used to improve the accuracy of the surrogates in given areas that can be difficult to model efficiently (discontinuities, steep slopes, etc.). In our implementation of the ADOE, the feature–learning aspect is supported by two different techniques: i) Model Error Sampling (MES), according to which multiple surrogate models are built over the domain and the areas of major interest are identified as those where the variance between these surrogate models is higher; and ii) Non–Linearity Search

(NLS), where the areas of major interest are identified by evaluating the misfit between the simulated output and the output estimated by means of a local linear approximation based on nearby samples.

A balanced strategy combining space– and feature–learning is adopted in the current ADOE methodology. The ADOE strategy, illustrated in Figure 4, consists of the following steps:

1. *Initialization.* An initial set of samples is drawn according to a traditional (non–adaptive) DOE technique.
2. *Build surrogate models.* A set of surrogate models is built according to the available simulation results and the regions of major interest are identified according to the MES and NLS algorithms.
3. *Adaptive sampling.* A new set of design points is chosen according to: i) the information obtained at Step 2; and ii) the trade–off strategy between space– and feature–learning that was chosen before running the algorithm.
4. *Check termination criteria.* If the termination criteria are not satisfied, a new batch of experiments is run and the algorithm restarts from Step 2. Suitable termination criteria may consist of: i) maximum number of model evaluation; or ii) accuracy of the surrogate models, measured in terms of misfit between the simulated outputs and the output calculated from the surrogate models. In the current implementation, this metric is calculated on the basis of an extra set of samples that are used exclusively for this purpose, called "validation set".

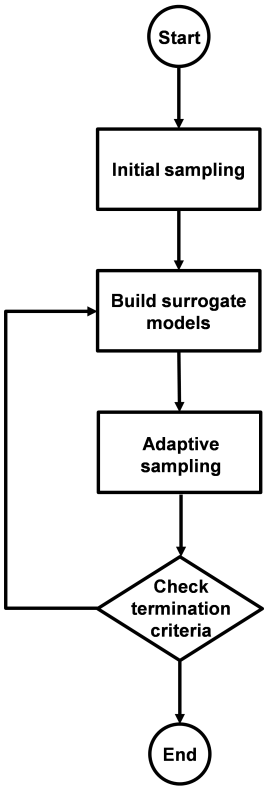

Figure 4: Schematic of the ADOE algorithm employed in this work

4.2. Latin–Hypercube Design

The LH design (LHD) is one of the most commonly used random DOE (12). A LHD is constructed by dividing the range of each design parameter in n equally probable intervals, n being the number of design points. The design points are then randomly chosen in such a way that for each interval there is only one design point. This selection of design points ensures that: i) each interval is present in the design; and ii) the number of levels is maximized. One of the main advantages of LHDs is that it avoids the "collapse problem", because if one or more of the input factors appear to be irrelevant, every point in the design still gives information about the influence of the other factors on the response. In this way, each time–consuming computer experiment adds useful information.

The intervals onto which each input dimension is subdivided may be assigned randomly or according to a custom rule. An efficient and effective way to construct a LHD is to assign the intervals in such a way that the resulting design is space–filling, i.e. the design points are spread out and do not cluster in one portion of the experimental region. In our implementation of LHD, we: i) measure the degree of spread of the design points by computing the minimal distance between two of its design points; and ii) choose the LHD which provides the maximum value of this metric. This strategy is generally referred to as maximin LHD (11).

5. Results

This section is organised as follows. Firstly, aerodynamic predictions are validated against available experimental data at wind tunnel conditions in

Section 5.1. Then, the proposed ADOE methodology is demonstrated in the context of a realistic flight envelope, as discussed in Section 5.2.

5.1. Validation at Wind Tunnel Flow Conditions

The validation is carried out at the operating wind tunnel conditions, $M = 0.117$ and $\mathrm{Re} = 0.778 \cdot 10^6$. The free–stream angle of attack is varied between -10.0 and 40.0 deg. Experimental data are available at a step in angle of attack of 2.0 deg, whereas simulations were performed for a smaller increment of 1.0 deg.

A preliminary study was conducted to ensure the results presented are fully converged. Two flow conditions were chosen, at 0.0 and 10.0 deg angle of attack. The independence on the number of inner iterations was assessed comparing the average value of aerodynamic coefficients in the last 1000 iterations at three relevant check points: after 5000, 7500, and 10000 iterations. The convergence of the residuals with the number of iterations is shown in Figure 5. The vertical lines in the figures indicate the intermediate check points at 5000 and 7500 iterations. The normal force and pitch moment coefficients, C_N and C_m, respectively, computed at 5000, 7500, and 10000 iterations are reported in Table 2. It was found that the percent error, computed using the values at 10000 iterations, is well below one percent in all cases. Based on this finding, all simulation results reported herewith were obtained for 5000 iterations.

The static aerodynamic characteristics are shown in Figure 6. Available wind tunnel measurements, referred to as "Exp Data" in figure, suggest that the normal force coefficient has a linear (or quasi–linear) behaviour with the angle of attack up to about 20 deg. Above this angle, the curve slope of the

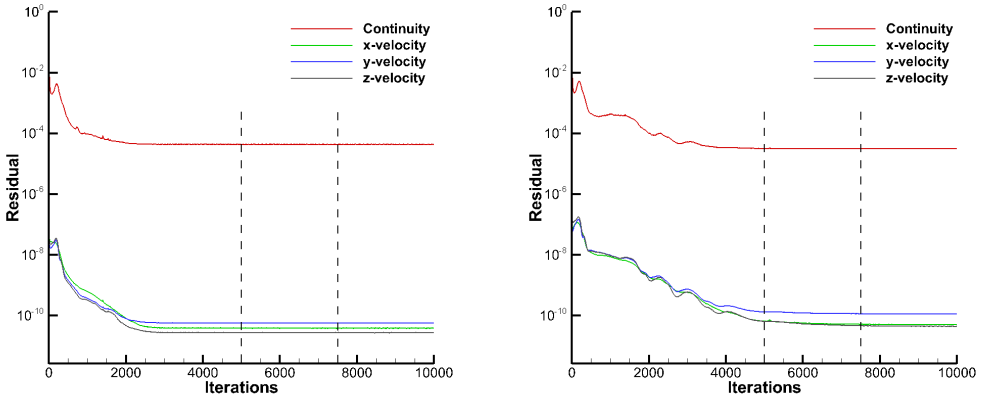

(a) $\alpha = 0.0$ deg (b) $\alpha = 10.0$ deg

Figure 5: Convergence of the solution residuals at two angles of attack at wind tunnel conditions ($M = 0.117$ and $\text{Re} = 0.778 \cdot 10^6$)

Table 2: Convergence of the aerodynamic loads with the number of iterations at wind tunnel conditions ($M = 0.117$ and $\text{Re} = 0.778 \cdot 10^6$)

	$\alpha = 0.0$ deg		$\alpha = 10.0$ deg	
Iterations	C_N	C_m	C_N	C_m
5000	$1.120 \cdot 10^{-1}$	$-9.110 \cdot 10^{-2}$	$6.435 \cdot 10^{-1}$	$-2.077 \cdot 10^{-1}$
7500	$1.120 \cdot 10^{-1}$	$-9.110 \cdot 10^{-2}$	$6.428 \cdot 10^{-1}$	$-2.070 \cdot 10^{-1}$
10000	$1.120 \cdot 10^{-1}$	$-9.110 \cdot 10^{-2}$	$6.427 \cdot 10^{-1}$	$-2.069 \cdot 10^{-1}$

force coefficient decreases, until the maximum value of normal force coefficient is found at about 38 deg. The pitch moment coefficient has a strong non–linear dependency on the angle of attack. Two break points are identified, at about 6 and 20 deg. For small angles of attack, the pitch moment coefficient has a negative slope, i.e. nose–down tendency for increasing angle of attack. A first break point is found at about 6 deg, where the slope sign changes to positive. Reference (9) attributed this to a continuously increasing lift on the canard wing, which is located upstream of the moment reference point and causes a nose–up tendency. The lightly unstable characteristics, confined between 6 and 20 deg, are then followed by a second break point, which suggests a massive flow separation.

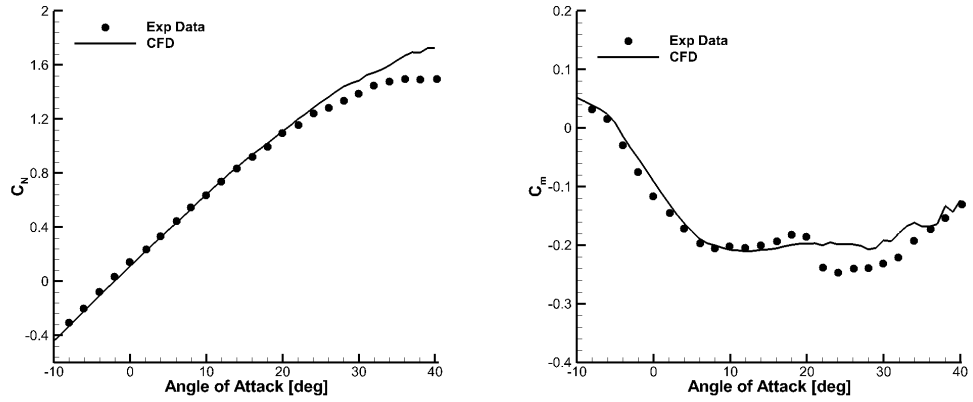

(a) Normal force coefficient (b) Pitch moment coefficient

Figure 6: Static aerodynamic characteristics of the TCR wind tunnel model at wind tunnel conditions ($M = 0.117$ and $\mathrm{Re} = 0.778 \cdot 10^6$)

The comparison of the CFD results against wind tunnel measurements is excellent up to about 20 deg, as in Figure 6. Aerodynamic characteristics are

well captured, including the normal force coefficient curve slope and the non–linear dependency of the pitch moment coefficient with the angle of attack. The reference point for the pitch moment coefficient is in close proximity with the location of the vortex breakdown on the main wing, which moves upstream for increasing angle of attack. Predictions of C_m are therefore very sensitive to the simulated flow features. The agreement indicates that the flow physics are simulated correctly with the turbulence model adopted up to about 20 deg. The surface signature and structure of the vortices forming over the canard and main wing are shown in Figure 7 for various angles of attack. Above $\alpha = 20.0$ deg, the flow presents massively separated regions that are not modelled properly with a RANS model, requiring higher fidelity in the flow modelling.

5.2. Aerodynamic Characteristics Across the Flight Envelope

To investigate the capability of the DOE techniques, a two–dimensional parameter space was generated, including representative variations of the angle of attack, α, and the Mach number, M. The Mach number range was set to $M \in [0.117, 0.970]$, whereas the lower and upper boundaries of the angle of attack are function of the Mach number: $\alpha \in [-5.0, 40.0]$ deg at $M = 0.117$, and $\alpha \in [0.0, 5.0]$ deg at $M = 0.97$. The two–dimensional parameter space is illustrated by the dashed line in Figure 8(a).

Since the DOE techniques are designed to work on rectangular domains, it is required to: i) sample the design points on a canonical square defined within the interval $[-1, 1]$ in both dimensions; and ii) map these points onto the physical domain by means of a bi–linear transformation. This is illustrated in Figure 8 for the parameter space of this study.

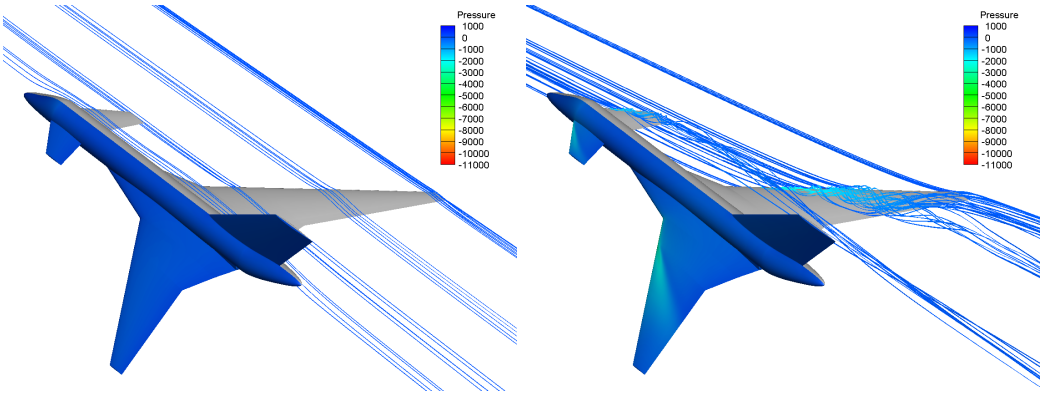

(a) $\alpha = 0.0$ deg

(b) $\alpha = 10.0$ deg

(c) $\alpha = 15.0$ deg

(d) $\alpha = 20.0$ deg

Figure 7: Flow visualisation using surface pressure distribution (in Pa) and volume streamtraces; for visualisation, the computational model was mirrored ($M = 0.117$ and $\mathrm{Re} = 0.778 \cdot 10^6$)

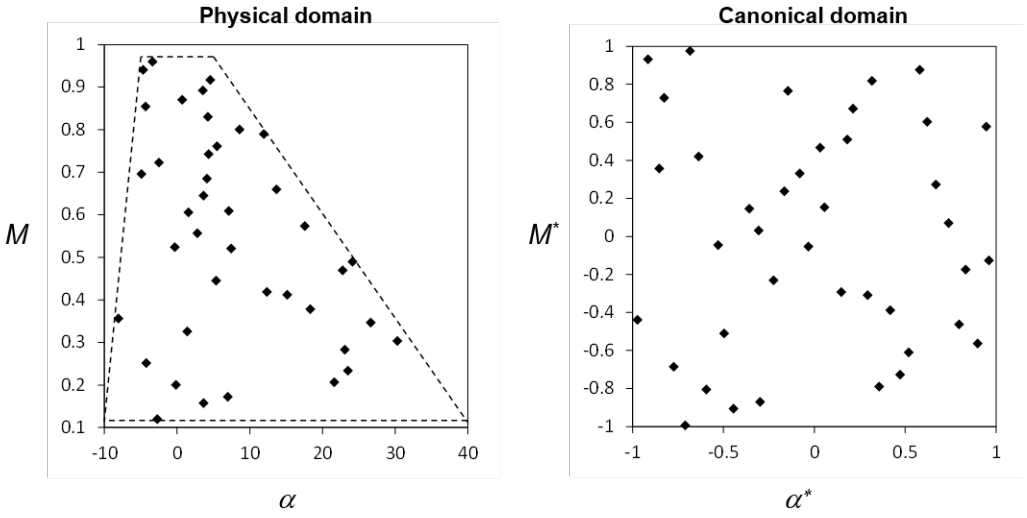

(a) Physical domain (b) Canonical domain

Figure 8: Bi–linear transformation mapping physical domain in (a) with canonical domain in (b); the parameters in (a) are angle of attack, α, and Mach number, M

As detailed in Section 4, the results obtained by running two DOE techniques, each being composed by 40 design points, are compared. The DOE methods are run using the algorithms implemented in the process integration and simulation framework "Noesis Optimus" (13). The software is also used to automate the submission of the CFD simulations to the IRIDIS HPC.

The ADOE strategy is initialized by calculating the output of a set of 10 experiments that are drawn using a LH technique. Then, the iterative procedure depicted in Figure 4 is started, and a new batch of 10 experiments is launched at each iteration until the total number of 40 experiments is reached.

The outputs obtained by running the two DOE algorithms are employed to build corresponding analytical surrogate models of C_N and C_m. In this study, the analysis is focused on one type of response surface model, i.e. radial basis function (RBF) – cubic. Figure 9 shows the behaviour of the surrogate models obtained from LH and ADOE experiments. It is found that the response surfaces obtained for C_N are virtually the same for both approaches. On the opposite, the surrogates of C_m have substantial differences and provide distinct predictions of the target quantity, especially in correspondence of the lower–right corner of the investigated domain (low speed, high angles of attack). These differences can be explained by the fact that the design points employed by the ADOE algorithm: i) are more uniformly distributed within the domain of interest, and ii) provide a better "coverage" of the area of the domains that are typically difficult to model (corners and boundaries).

The enhanced capability of the ADOE algorithm with respect to LH to distribute the design points in an intelligent way is also reflected in an

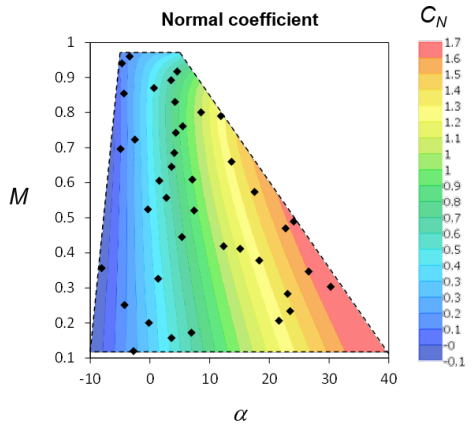

(a) Normal force coefficient/LH

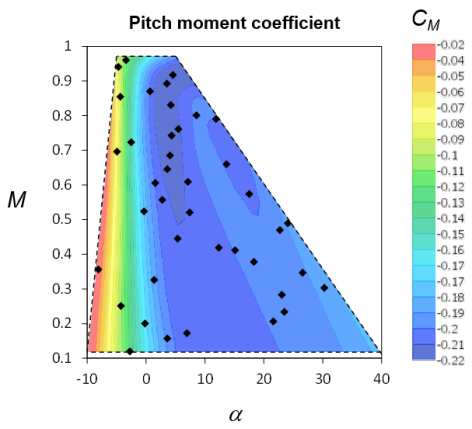

(b) Pitch moment coefficient/LH

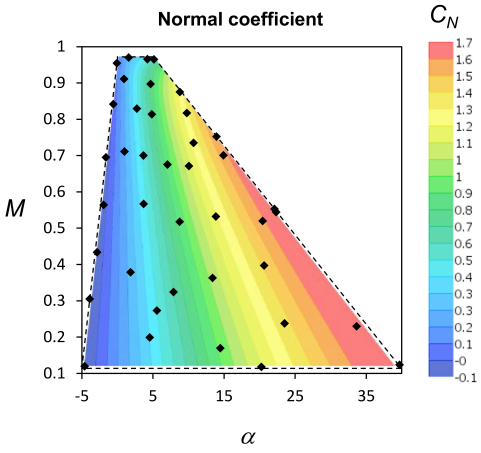

(c) Normal force coefficient/ADOE

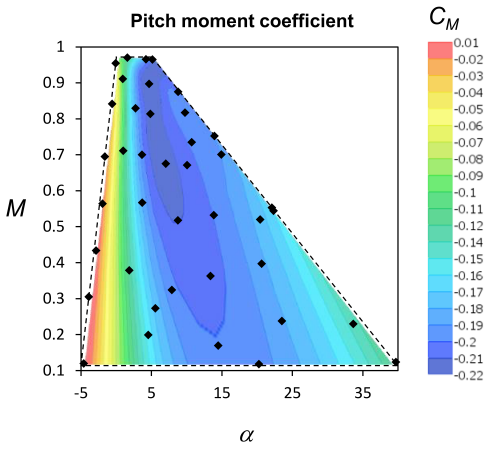

(d) Pitch moment coefficient/ADOE

Figure 9: Surrogate model resulting from the interpolation of the outputs associated with: in (a), the 40 LH experiments using a RBF – cubic interpolating model; and in (b), the 40 ADOE experiments

improved quality of the predictions obtained from the associated surrogate models. To quantify this, an additional batch of 66 experiments were run for validating the quality of the surrogate models shown in Figure 9. Twenty validation points are distributed within the domain by means of a LH algorithm while the remaining 46 points correspond to the experiments used to validate the CFD model (recall Section 5.1 and, in particular, Figure 6). The data corresponding to the wind tunnel operating conditions are particularly useful to test the ability of the surrogate models to predict the true output in the correspondence of the domain boundary. The scatter plots depicted in Figure 10 compare the outputs calculated by the surrogate models and by CFD calculation in the correspondence of the 66 validation points. The predictive capability of each response surface model is measured in terms of the sum of the squared error (SSE). In the figures, the dashed diagonal line indicates a perfect match between the surrogate model prediction and the CFD data. In the case of a perfect match, the SSE is zero. The scatter plots demonstrate that the surrogate models built upon the ADOE experiments are able to provide a better prediction of the system response. This difference is particularly evident by comparing the pitch moment coefficient in Figures 10(b) and 10(d). In Figure 10(d), data are well aligned along the dashed diagonal line, indicating a smaller error to the CFD results than achieved by the surrogate model built using the LH experiments. This is quantified in terms of SSE: the SSE value obtained from ADOE algorithm ($SSE = 0.03$) is nearly one order of magnitude lower than the same quantity calculated from the LH algorithm ($SSE = 0.10$).

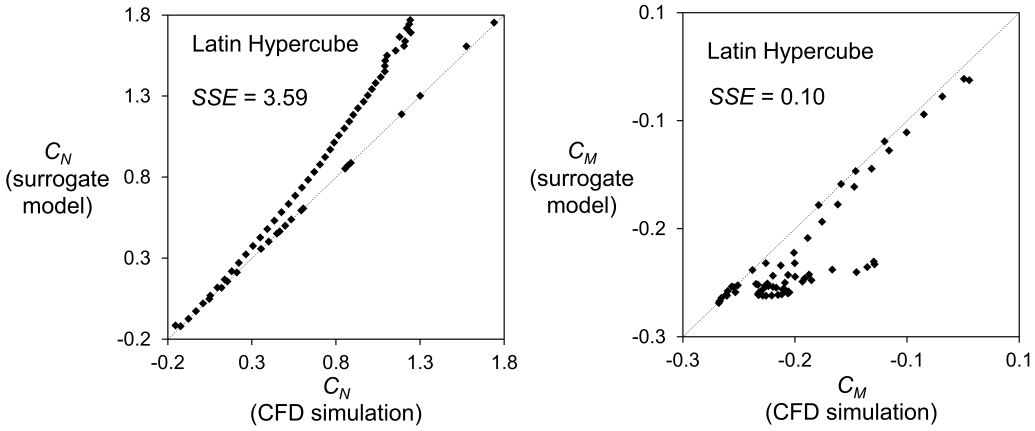

(a) Normal force coefficient/LH (b) Pitch moment coefficient/LH

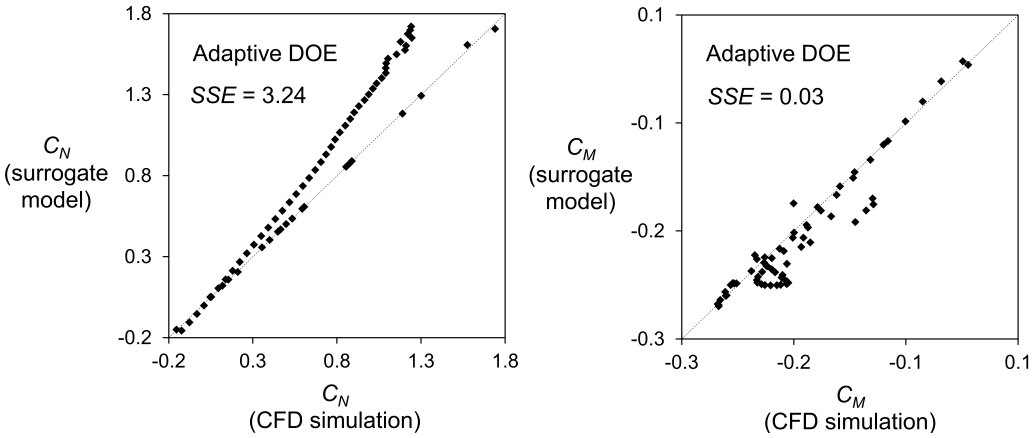

(c) Normal force coefficient/ADOE (d) Pitch moment coefficient/ADOE

Figure 10: Scatter plots obtained by comparing the outputs calculated from CFD calculations and those evaluated on the basis of the response surface models of the two output variables (C_N and C_m) for each DOE algorithm at the 66 validation points

6. Conclusions

The work carried out in this study investigates an efficient and effective methodology to generate a full aerodynamic database for a complete aircraft model. The Reynolds–averaged Navier–Stokes equations are solved on a grid containing approximately 10 million points. Preliminary tests confirmed that results were independent of the grid spatial discretisation. To build confidence on the accuracy of the numerical results using the one–equation Spalart–Allmaras turbulence model, results were compared to available wind tunnel data measured at a Mach number of 0.117 and Reynolds number of 0.778 million. An excellent agreement was found for both normal force and pitch moment coefficients up to 20 degree angle of attack. The numerical challenges include: i) the prediction of the separation lines at the wind tunnel speed around lifting surfaces with a round leading edge, which is still an open issue in computational fluid dynamics; ii) interacting vortices and their coalescence; and iii) the high computational costs associated with a single analysis, which make the generation of a full aerodynamic database unrealistic on a manageable time scale.

Having verified that numerical results using a spatially converged grid are in good agreement with experimental data, a two–dimensional flight envelope was created. The design parameters are for the angle of attack and Mach number. The angle of attack varies with Mach number, and the range reduces for increasing Mach number. A surrogate model, based on radial basis function interpolation, was used to approximate the aerodynamic loads across the flight envelope from a total of 40 numerical results. To distribute the 40 experiments, two design of experiments strategies were investigated.

The first one is a traditional latin hypercube approach whereby samples are randomly distributed throughout the parameter space. The second strategy is based on an adaptive design of experiments technique. This iterative technique analyses data produced in previous iterations in order to distribute the design points of the next iteration in areas of the parameters space considered of interest only.

To assess the accuracy of the two surrogate models, measured in terms of misfit between the numerical results using the Spalart–Allmaras turbulence model and the output of the surrogate model, an extra set of samples were used. The extra set of samples include 20 points distributed within the domain by means of a latin hypercube algorithm while the remaining 46 points are for the lowest Mach number, coinciding with the wind tunnel measurements. The data corresponding to the wind tunnel operating conditions are particularly useful to test the ability of the surrogate models to predict the true output in the correspondence of the domain boundary.

The predictive capability of each response surface model is measured in terms of the sum of the squared error. In the case of a perfect match between the surrogate model prediction and the Reynolds–averaged Navier–Stokes data, the sum of the squared error is zero. It was found that the surrogate model built upon the adaptive strategy is able to provide a better prediction of the system response. This, in particular, is valid for the pitch moment coefficient that shows strong non–linear features. Quantitatively, the sum of the squared error value obtained from adaptive algorithm ($SSE = 0.03$) is nearly one order of magnitude lower than the same quantity calculated from the latin hypercube algorithm ($SSE = 0.10$). Conversely, the surro-

gate model built using the latin hypercube algorithms requires more samples (and more expensive calculations) to achieve the same error level than the surrogate model using the adaptive algorithm.

This study demonstrates that a surrogate model built upon an adaptive design of experiments strategy achieves a higher prediction capability than that built upon a traditional strategy. Two instrumental considerations are that: i) the adaptive strategy does not incur in extra costs compared to the traditional counterpart, and ii) the integration within an existing environment is seamless. The authors hope this demonstration will facilitate the adoption of the adaptive design of experiments methodology in the analysis of other complex and non–linear engineering phenomena.

Competing Interests

The authors declare that they have no competing interests.

Acknowledgements

The authors acknowledge the use of the IRIDIS High Performance Computing Facility, and associated support services at the University of Southampton, in the completion of this work. Andrea Da Ronch is also grateful for the financial support received from the Royal Academy of Engineering under the Industrial Secondments Scheme (ISS1415\7\44). The authors also acknowledge the contribution from the following people: Adam Jirasek of the USAF who provided the grid of the TCR model; and Maximilien Landrain of Noesis Solutions N. V. and Elena Vataga of the University of Southampton for the deployment of Noesis Optimus on IRIDIS.

References

[1] T. J. Mackman, C. B. Allen, M. Ghoreyshi, K. J. Badcock, Comparison of adaptive sampling methods for generation of surrogate aerodynamic model, AIAA Journal 51 (4) (2013) 797–808, doi: 10.2514/1.J051607.

[2] A. Da Ronch, M. Ghoreyshi, K. J. Badcock, On the generation of flight dynamics aerodynamic tables by computational fluid dynamics, Progress in Aerospace Sciences 47 (8) (2011) 597–620, doi: 10.1016/j.paerosci.2011.09.001.

[3] M. Ghoreyshi, R. M. Cummings, A. Da Ronch, K. J. Badcock, Transonic aerodynamic loads modeling of X–31 aircraft pitching motions, AIAA Journal 51 (10) (2013) 2447–2464, doi: 10.2514/1.J052309.

[4] A. Rizzi, Modeling and simulating aircraft stability and control – the SimSAC project, Progress in Aerospace Sciences 47 (8) (2011) 573–588, doi: 10.1016/j.paerosci.2011.08.004.

[5] A. Rizzi, P. Eliasson, T. Goetzendorf-Grabowski, J. B. Vos, M. Zhang, T. S. Richardson, Design of a canard configured transcruiser using CEASIOM, Progress in Aerospace Sciences 47 (8) (2011) 695–705, doi: 10.1016/j.paerosci.2011.08.011.

[6] A. N. Khrabrov, K. A. Kolinko, Y. A. Vinogradov, A. N. Zhuk, I. I. Grishin, I. D. I., Experimental investigation and mathematical simulation of unsteady aerodynamic characteristics of a transonic cruiser model at small velocities in a wide range of angles of attack, Visualization

of Mechanical Processes: An International Online Journal 1 (2), doi: 10.1615/VisMechProc.v1.i2.40.

[7] D. Vallespin, A. Da Ronch, O. Boelens, K. J. Badcock, Validation of vortical flow predictions for a UCAV wind tunnel model, Journal of Aircraft 48 (6) (2011) 1948–1959, doi: 10.2514/1.C031385.

[8] A. Da Ronch, D. Vallespin, M. Ghoreyshi, K. J. Badcock, Evaluation of dynamic derivatives using computational fluid dynamics, AIAA Journal 50 (2) (2012) 470–484, doi: 10.2514/1.J051304.

[9] B. Mialon, A. Khrabrov, S. B. Khelil, A. Huebner, A. Da Ronch, K. J. Badcock, L. Cavagna, P. Eliasson, M. Zhang, S. Ricci, J.-C. Jouhaud, G. Rogé, S. Hitzel, M. Lahuta, Validation of numerical prediction of dynamic derivatives: the DLR–F12 and the transcruiser test cases, Progress in Aerospace Sciences 47 (8) (2011) 674–694, doi: 10.1016/j.paerosci.2011.05.002.

[10] P. R. Spalart, S. R. Allmaras, A one equation turbulence model for aerodynamic flows, in: 30th Aerospace Sciences Meeting and Exhibit, AIAA Paper 1992–439, 1992, doi: 10.2514/6.1992-439.

[11] M. E. Johnson, L. M. Moore, D. Ylvisaker, Minimax and maximin distance designs, Journal of Statistical Planning and Inference 26 (2) (1990) 131–148, doi: 10.1016/0378-3758(90)90122-B.

[12] M. D. McKay, R. J. Beckman, W. J. Conover, A comparison of three methods for selecting values of input variables in the analysis of out-

put from a computer code, Technometrics 42 (1) (2000) 55–61, doi: 10.2307/1271432.

[13] Optimus rev 10.17 – manual, Noesis Solutions (September 2015).